References

[1]Buning, P., Jespersen, D. C., Pulliam, T. H., Chan, W. M., Slotnick, J. P., Krist, S. E., and Renze, K. J., *OVERFLOW User's Manual*, Ver. 1.7v, NASA Ames Research Center, Moffet AFB, CA, 1995.

[2]Tuncer, I. H., and Platzer, M. F., "Computational Study of Subsonic Flow over a Close-Coupled Delta Canard-Wing-Body Configuration," *Journal of Aircraft*, Vol. 35, No. 4, 1998, pp. 554–560.

[3]Tuncer, I. H., Platzer, M. F., and VanDyken, R. D., "Navier–Stokes Analysis of Subsonic Flowfields over a Missile Configuration," *Journal of Spacecraft and Rockets*, Vol. 35, No. 2, 1998, pp. 127–131.

[4]Tuncer, I. H., and Platzer, M. F., "Computational Investigation of Flow Through a Louvered Inlet Configuration," AIAA Paper 01–2477, June 2001.

Angle-of-Attack Effect on Transonic/ Supersonic Aeroelasticity of Wing-Box Model

Jae-Han Yoo,* Dong-Hyun Kim,† and In Lee‡

Korea Advanced Institute of Science and Technology, Taejon 305-701, Republic of Korea

Introduction

AN understanding of the aeroelastic behavior of flight vehicles in the transonic and low-supersonic regimes is of great importance for flight safety. The flutter boundary in this regime varies with changes in the initial angle of attack. Aeroelastic analyses and experiments on the effect of initial angle of attack have been performed previously. Early studies of the two-degree-of freedom airfoil system were performed using the HYTRAN2 (Ref. 1) and an Euler code.[2] For a three-dimensional wing at high angles of attack in incompressible flow, there is the work by Strganac and Mook.[3] In their paper, using the unsteady vortex-lattice method, the equations of motion were integrated, considering the nonlinear effects of the separated vortex. Yates et al.[4] analyzed the effect of angle of attack on a large aspect ratio transport-type wing with a supercritical airfoil, using a modified strip analysis employing wind-tunnel steady aerodynamic data. Also, the CAP-TSD code[5] has been applied to the active flexible wing wind-tunnel model to investigate static and dynamic aeroelastic behaviors below Mach 0.95. These studies provide a good foundation for understanding initial angle-of-attack effects, both theoretically and practically, and motivated by this, we will examine in detail the effect of both positive and negative angles of attack on a typical fighter wing-box model with an asymmetric airfoil in the transonic and low-supersonic flow regions. The critical effect of a negative angle of attack and unusual frequency changes due to the effect of normal shocks are presented. The computed steady aerodynamic results for rigid and deformed shapes of the model are presented and compared. Also, detailed dynamic aeroelastic responses are computed using a coupled time-marching method based on the effective computational structural dynamic (CSD) and computational fluid dynamic (CFD) techniques,[6] which are similar to those used in Ref. 5. CSD analyses for the wing-box model have been performed using MSC/NASTRAN. The variations of flutter boundary due to the change of initial angles of attack are also compared for several Mach numbers.

Received 10 December 2001; revision received 20 May 2002; accepted for publication 20 May 2002.

*Graduate Research Assistant, Department of Aerospace Engineering, 373-1 Kusong-dong, Yusong-gu.

†Postdoctoral Research Associate, Department of Aerospace Engineering, 373-1 Kusong-dong, Yusong-gu. Member AIAA.

‡Professor, Department of Aerospace Engineering, 373-1 Kusong-dong, Yusong-gu. Senior Member AIAA.

Computational Method

The aeroelastic equations of motion for an elastic wing can be formulated in terms of generalized displacement response vector $\{q(t)\}$, which is a solution of the following equation:

$$[M_g]\{\ddot{q}(t)\} + [C_g]\{\dot{q}(t)\} + [K_g]\{q(t)\} = \{Q(t, q, \dot{q})\} \quad (1)$$

where $[M_g]$ is the generalized mass matrix, $[C_g]$ is the generalized damping matrix, and $[K_g]$ is the generalized stiffness matrix. $\{Q\}$ is the vector of generalized aerodynamic forces computed by integrating the pressure distributions on the wing surface as

$$Q(t)_i = \frac{1}{2}\rho U^2 c_r^2 \iint_S \left[C_{p_L}(x, y, t) - C_{p_U}(x, y, t)\right]\psi_i(x, y)\frac{dS}{c_r^2} \quad (2)$$

where ρ is the freestream air density; U is the freestream velocity; c_r is the reference chord length; S is the wing area; C_p is the unsteady pressure coefficient on the arbitrary wing surface; the subscripts L and U refer to the lower and upper surface, respectively; and

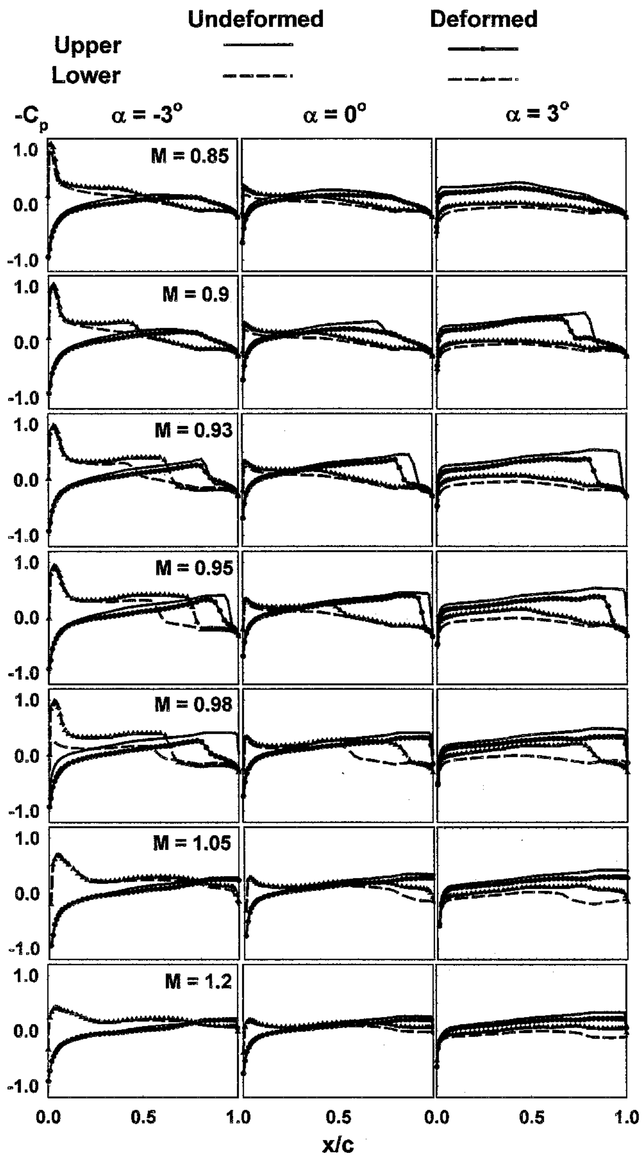

Fig. 1 Comparison of steady pressure coefficients between rigid and elastic wing (shown at the midspan station).

ψ_i is the ith mode shape. To perform the numerical integration of Eq. (2), a two-point formula of Gaussian quadrature is used for each aerodynamic grid cell on the wing surface. In this study, to consider the characteristics of aeroelastic responses, the coupled time integration method has been used. Practically speaking, the damping matrix $[C_g]$ for each mode is assumed as $2\zeta_i\omega_i$, based on the proportional damping concept. To get the converged static aeroelastic solution rapidly, ζ is artificially assumed as 0.95 for each angle of attack. The detailed numerical process for aeroelastic computations used in this study is very similar to those described in Refs. 5 and 6. Also, the computational results for steady and unsteady aerodynamic analyses using the present TSD 3KR code are seen from Ref. 7.

Results and Discussion

The typical wing-box model considered here has a wing aspect ratio of 3.0, taper ratio of 0.23, and a swept-back angle at the leading edge of 40 deg. The wing section is assumed to be a 64A204 airfoil, and there is no aerodynamic twist. The aerodynamic root chord length is 160 in., and it is the same structural model used in Ref. 6, except for the tip launcher and missile. The full computational mesh used is a $75(x) \times 32(y) \times 40(z)$ grid, where 50 chordwise and 22 spanwise grid points were used on the aerodynamic wing surface.

Figure 1 shows the comparisons of steady pressure coefficients between the rigid and the deformed wings at the midspan station for several Mach numbers. The initial angles of attack considered here are −3, 0, and +3 deg, unless otherwise stated, and the flight altitude is considered to be 5000 ft. For these moderate angle-of-attack conditions, it is assumed that transonic small disturbance theory can accurately predict the steady and unsteady flowfields. The dynamic pressures used at each Mach number correspond to flutter conditions. The strong normal shocks on the upper and lower surfaces can be clearly seen at high-transonic Mach numbers of 0.9, 0.93, 0.95, and 0.98. The pressure distributions for rigid and elastic wings are different, even though at a zero angle of attack, because the wing has an asymmetric airfoil with positive camber. Note that in the high-transonic region there are large changes of shock positions between the rigid and elastic wings, but not in the low-transonic and high-supersonic regions. In the transonic region, the steady shock on the upper surface moves forward for both positive and negative angles of attack after deformation resulting from static aeroelastic effects. For this model, the aeroelastic deformation of the wing shape exhibits a nosedown rotation or washout effects.

Figure 2 represents comparisons of spanwise lift distributions between rigid and elastic wings. We can see that the lift coefficients of the elastic wing can be changed considerably by the structural deformations due to the typical washout effect of a swept-back angle. It also shows that the variation of spanwise lift coefficients are larger than in the case of zero angle of attack at $M = 0.95$. This result may be also expected from the large variation of shock positions as presented in Fig. 1. At Mach 1.2, the variation of spanwise lift for negative angle of attack is relatively small and dominant at the wing tip region.

To consider the physical dynamic characteristics, the detailed aeroelastic responses of wing tip trailing edge are compared for several Mach numbers, as shown in Fig. 3. All of the responses are found to be neutrally stable conditions corresponding to the flutter velocity presented in Fig. 4. An artificial modal damping ratio of 0.95 is assumed in the equations of motion to achieve a fast static convergence and are then removed after 0.3 s. The first and second modal velocities are applied as initial disturbances. It is shown that as the angle of attack increases, the mean value of the converged static aeroelastic responses of the wing tip also increases. At Mach 0.85, 0.9, and 1.2, the magnitudes and frequencies of aeroelastic responses are almost identical for different angles of attack. Note, however, that amplitude and frequency are different for a high transonic Mach number of 0.95 because of the change of the dominant flutter mode shape.

Figure 4 shows the comparison of computed flutter velocity and frequency. The flutter velocities and frequencies are normalized by the reference value of Mach 0.7 at $\alpha_0 = 0$ deg. The flutter dip regions are observed at the flight conditions of $M = 0.95$ at $\alpha_0 = 0$ deg and $M = 0.92$ at $\alpha_0 = -3$ deg. For positive angles of attack such as $\alpha_0 = 3$ deg, the flutter dip regions show improved flutter stability when compared with the zero-angle-of-attack case. These different effects for positive and negative angles of attack are mainly due to the effect of the asymmetric airfoil shape with positive camber. However, the effect of moderate angles of attack seems to be very trivial for the supersonic flow region. The effect of negative angles of attack tend to be much more important for the flutter stability in this case.

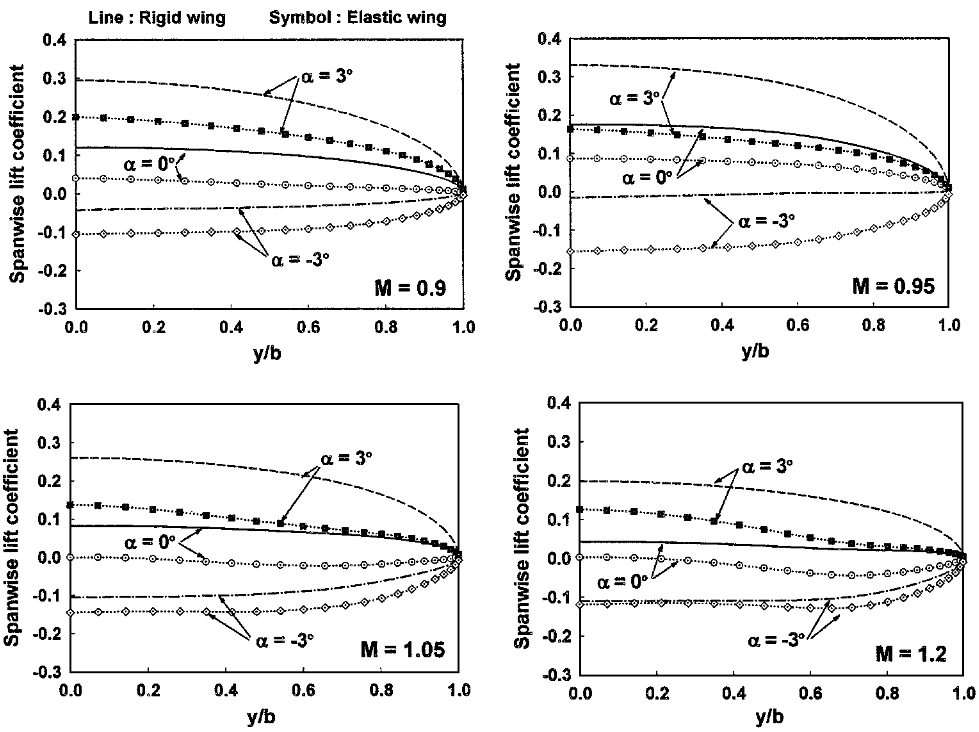

Fig. 2 Spanwise lift distributions of rigid and elastic wings.

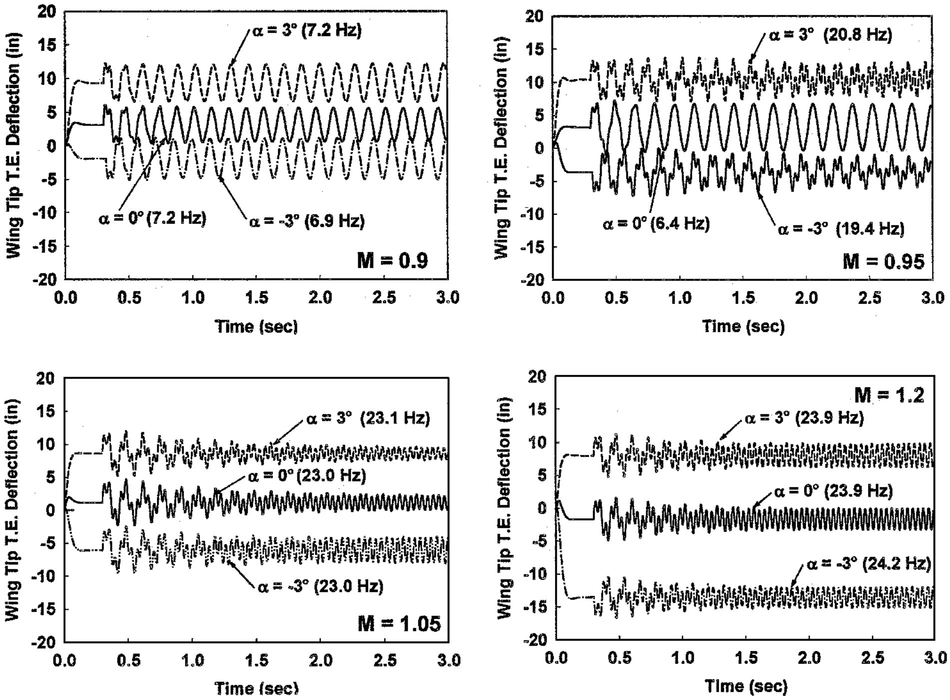

Fig. 3 Time-marching aeroelastic responses of elastic wing (shown for wing tip trailing edge).

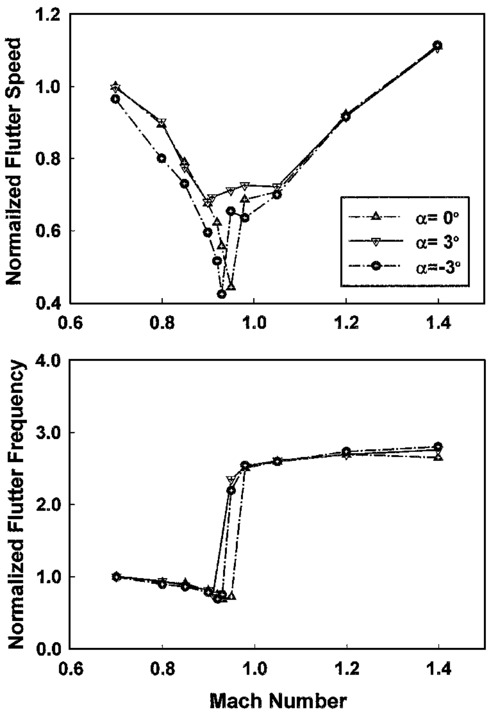

Fig. 4 Comparisons of flutter velocity and frequency vs. Mach number for various angles of attack.

Conclusions

The present study considered the nonlinear aeroelastic phenomena of a swept-back wing-box model with moderate initial angles of attack in the transonic and low-supersonic flow regions. A coupled CFD and CSD technique was applied to analyze static and dynamic aeroelasticity. For various angles of attack, static aeroelastic analyses were performed, and then the effects of elastic deformation on the shock were studied. In the transonic region, there are large changes of aerodynamic characteristics due to the effect of static deformation with initial angles of attack. The effects of angle of attack on the flutter boundary were also studied, and the detailed dynamic responses are presented. The results typically show that, for the high-transonic region such as $M = 0.95$, an initial angle of attack can induce a change in the dominant flutter mode and flutter frequency, resulting in a change of flutter speed. Also note that the airfoil camber plays an important role in flutter stability, combined with the effect of initial angle of attack and shock wave location.

Acknowledgment

This work was supported through funding from the Republic of Korea Ministry of Science and Technology. The authors would like to acknowledge the support (Subject 2000-N-NL-01-C-250) of the National Research Laboratory Program.

References

[1]Edwards, J. W., Bennett, R. M., Whitlow, W., Jr., and Seidel, D. A., "Time-Marching Transonic Flutter Solutions Including Angle-of-Attack Effects," *Journal of Aircraft*, Vol. 20, No. 11, 1983, pp. 899–906.

[2]Reddy, T. S. R., and Srivastava, R., "Effects of Rotational Flow, Viscosity, Thickness, and Shape on Transonic Flutter Dip Phenomena," AIAA Paper 88-2348, 1988.

[3]Strganac, T. W., and Mook, D. T., "Application of the Unsteady Vortex-Lattice Method to the Nonlinear Two-Degree-of-Freedom Aeroelastic Equations," AIAA Paper 86-0687, May 1986.

[4]Yates, E. C., Jr., Wynne, E. C., and Farmer, M. G., "Effect of Angle of Attack on Transonic Flutter of a Supercritical Wing," *Journal of Aircraft*, Vol. 20, No. 10, 1983, pp. 841–847.

[5]Silva, W. A., "Using Transonic Small Disturbance Theory for Predicting the Aeroelastic Stability of a Flexible Wind-Tunnel Model," AIAA Paper 90-1033, 1990.

[6]Kim, D. H., and Lee, I., "Transonic and Supersonic Flutter Characteristics of a Wing-Box Model with Tip Stores," AIAA Paper 2001-1464, 2001.

[7]Kim, D. H., and Lee, I., "Transonic and Low-Supersonic Aerodynamic Analysis of a Wing with Underpylon/Store," *Journal of Aircraft*, Vol. 37, No. 1, 2000, pp. 189–192.